PHYSICAL REVIEW D **93,** 093003 (2016)

CP-violating phase in a two Higgs triplet scenario: Some phenomenological implications

Avinanda Chaudhuri* and Biswarup Mukhopadhyaya†

Regional Centre for Accelerator-based Particle Physics, Harish-Chandra Research Institute, Chhatnag Road, Jhusi, Allahabad 211 019, India

(Received 3 March 2016; published 3 May 2016)

We consider a scenario where, along with the usual Higgs doublet, two scalar triplets are present. The extension of the triplet sector is required for the Type II seesaw mechanism for the generation of neutrino masses, if this mechanism has to generate a neutrino mass matrix with two-zero texture. One *CP*-violating phase has been retained in the scalar potential of the model, and all parameters have been chosen consistently with the observed neutrino mass and mixing patterns. We find that a large phase ($\gtrsim 60°$) splits the two doubly charged scalar mass eigenstates wider apart, so that the decay $H_1^{++} \to H_2^{++} h$ is dominant (with h being the 125 GeV scalar). We identify a set of benchmark points where this decay dominates. This is complementary to the situation, reported in our earlier work, where the heavier doubly charged scalar decays as $H_1^{++} \to H_2^{+} W^{+}$. We point out the rather spectacular signal, ensuing from $H_1^{++} \to H_2^{++} h$, in the form of Higgs plus the same-sign dilepton peak, which can be observed at the Large Hadron Collider.

DOI: 10.1103/PhysRevD.93.093003

I. INTRODUCTION

The observation of a rather distinctive pattern of neutrino mixing, together with the available information on neutrino mass splitting, has triggered numerous theoretical proposals going beyond the standard electroweak model (SM). Seesaw models enjoy a fair share of these, along with additional assumptions to suit particular textures of the neutrino mass matrix.

Type-II seesaw models can generate Majorana neutrino masses without any right-handed neutrino(s), with the help of one or more $Y = 2$ scalar triplets. The restriction of the vacuum expectation value (VEV) of such a triplet, arising from the limits on the ρ-parameter (with $\rho = m_W^2/m_Z^2\cos^2\theta$), is obeyed in a not so unnatural manner, where the constitution of the scalar potential can accommodate large triplet scalar masses *vis-à-vis* a small VEV. In fact, this very feature earns such models classification as a type of "seesaw."

A lot of work has been done on the phenomenology of scalar triplets which, interestingly, also arise in left-right symmetric theories [1]. One can, however, still ask the question: is a single-triplet scenario self-sufficient, or does the replication of triplets (together with, say, the single scalar doublet of the SM) bring about any difference in phenomenology? This question, otherwise a purely academic one, acquires special meaning in the context of some neutrino mass models which aim to connect the mass ordering with the values of the mixing angles, thereby achieving some additional predictiveness. One class of such models depends on texture zeros, where a number of zero entries (usually restricted to two) in the mass matrix enable one to establish the desired connection. The existence of such zero entries require the imposition of some additional symmetry; it has, for example, been shown that a horizontal $\mathcal{Z}_4$ symmetry can serve the purpose. The simultaneous requirement of zero textures and the Type-II seesaw mechanism [2], however, turns out to be inconsistent, as has been discussed in earlier works [3]. The inconsistency is gone for two or more triplets. This resurrects the relevance of the phenomenology of two-triplet, one-doublet scalar sectors, this time with practical implications. We have studied such phenomenology in Ref. [4]. An important conclusion of this study was that, whereas the doubly charged scalar in the single triplet scenario would decay mostly in the $\ell^{\pm}\ell^{\pm}$ or $W^{\pm}W^{\pm}$ modes, the decay channel $H_1^{++} \longrightarrow H_2^{+} W^{+}$ acquires primacy over a large region of the parameter space. Some predictions on this in the context of the Large Hadron Collider were also shown in Ref. [4]. However, an added possibility with two triplets is the possibility of at least one *CP*-violating phase being there. This in principle can affect the phenomenology of the model, which is worth studying.

With this in view, we have analyzed here the one-doublet, two-triplet framework, including *CP*-violating effects arising via a relative phase between the triplets. Thus, the VEV of one triplet has been made complex, and consequently, the coefficient of the corresponding trilinear term in the scalar potential has also been rendered complex.

Indeed, the introduction of a phase results in some interesting findings that were not present when the relative phase was absent. First of all, as a result of mixing between two triplets and the presence of a relative phase between them, something on which no phenomenological

*avinanda@hri.res.in
†biswarup@hri.res.in

restrictions exits, the heavier doubly charged scalar can dominantly decay into the lighter doubly charged scalar plus the SM-like Higgs boson, i.e. $H_1^{++} \to H_2^{++} h$, over a larger range of parameter space. This can give rise to a spectacular signal in the context of the LHC. Basically, as a final state, we obtain $H_1^{++} \to \ell^+\ell^+ h$, i.e. a doubly charged scalar decaying into two same-sign leptons plus the SM-like Higgs. This decay often dominates over all other decay channels. When this decay is not present due to insufficient mass difference between respective scalars, the decay $H_2^{++} \longrightarrow H_2^+ W^+$ mostly dominates, and its consequence was discussed in some detail in our earlier work [4] on the *CP*-conserving scenario.

Second, for some combination of parameters, the decays mentioned in the above paragraph are not possible with a vanishing or small phase, due to an insufficient gap in masses between the respective scalars. However, if we continuously increase the value of the phase, keeping all the other parameters fixed, the mass differences between the scalars start to increase, so that the aforementioned channel finally opens up.

Third, we have noticed in [4] that the gauge coupling dominated decay $H_1^{++} \to H_2^+ W^+$ dominates over the Yukawa coupling dominated decay $\Delta^{++} \to \ell^+\ell^+$, even in those regions of parameter space where we have chosen the Yukawa coupling matrices to be sufficiently large ($\simeq 1$). On the other hand, the *CP*-violating phase suppresses the neutrino mass matrix elements for the same value of the triplet VEVs. This in turn requires an increase in the corresponding Yukawa coupling matrix elements, since the VEVs and Yukawa couplings are related by the expression for neutrino masses. The outcome of this whole process is that, for several benchmark points (BPs), the decay $H_1^{++} \to \ell^+\ell^+$ competes with the decay into $H_2^+ W^+$.

Finally, the *CP*-conserving scenario marks out regions of the parameter space, where the branching ratios of the decays $H_1^{++} \longrightarrow \ell^+\ell^+$ and $H_1^{++} \to W^+W^+$ are of comparable, though subdominant, rates. As the phase picks up, the same VEV necessitates a hike in Yukawa coupling, as discussed above. In such situations, the decay $H_1^{++} \to \ell^+\ell^+$ mostly dominates over the W^+W^+ mode.

Since, to the best of our knowledge, very little has been written on *CP*-violating phase(s) in two-triplet scenarios, we introduce the issue in a minimalistic manner, introducing one such phase. The presence of additional phases can of course subject the allowed parameter space to new possibilities. We postpone their discussion for a further study.

We present a summary of the scenario with a single triplet with complex VEV in Sec. II. In Sec. III, we outline the two-triplet scenario with a complex phase, including the corresponding scalar potential. The composition of physical states, the benchmark points for our numerical study and the results are presented in Sec. IV. We summarize and conclude in Sec. V.

II. A SINGLE SCALAR TRIPLET WITH A *CP*-VIOLATING PHASE

We first give the reader a glimpse of the scenario with a single triplet $\Delta = (\Delta^{++}, \Delta^+, \Delta^0)$, over and above the usual Higgs doublet ϕ, using the notation of [5]. Δ is equivalently denoted by the 2×2 matrix

$$\Delta = \begin{pmatrix} \Delta^+ & \sqrt{2}\Delta^{++} \\ \sqrt{2}\Delta^0 & -\Delta^+ \end{pmatrix}. \tag{1}$$

The VEVs of the doublet and the triplet are expressed as

$$\langle \phi \rangle_0 = \frac{1}{\sqrt{2}} \begin{pmatrix} 0 \\ v \end{pmatrix} \quad \text{and} \quad \langle \Delta \rangle_0 = \begin{pmatrix} 0 & 0 \\ v_T & 0 \end{pmatrix}, \tag{2}$$

respectively. The only doublet-dominated physical state that survives after the generation of gauge boson masses is a neutral scalar h.

The most general scalar potential including ϕ and Δ can be written as

$$\begin{aligned} V(\phi, \Delta) = {} & a\phi^\dagger\phi + \frac{b}{2}\mathrm{Tr}(\Delta^\dagger\Delta) + c(\phi^\dagger\phi)^2 + \frac{d}{4}(\mathrm{Tr}(\Delta^\dagger\Delta))^2 \\ & + \frac{e-h}{2}\phi^\dagger\phi\mathrm{Tr}(\Delta^\dagger\Delta) + \frac{f}{4}\mathrm{Tr}(\Delta^\dagger\Delta^\dagger)\mathrm{Tr}(\Delta\Delta) \\ & + h\phi^\dagger\Delta^\dagger\Delta\phi + (t\phi^\dagger\Delta\tilde{\phi} + \mathrm{H.c.}), \end{aligned} \tag{3}$$

where $\tilde{\phi} \equiv i\tau_2\phi^*$. All parameters in the Higgs potential are real except t which is complex in general. By performing a global $U(1)$ transformation, v can always be chosen real and positive. Because of the t-term in the potential there is no second global symmetry to make v_T real. Furthermore, t can also be complex and, therefore, it can be written as $t = |t|e^{i\alpha}$ and $v_T = we^{i\gamma}$ with $w \equiv |v_T|$. Minimization of the scalar potential with respect to the phase of v_T, i.e. γ, gives the relation between the phases as $\alpha + \gamma = \pi$.[1]

The choice $a < 0$, $b > 0$ ensures that the dominant source of spontaneous symmetry breaking is the scalar doublet. It is further assumed, following [5], that

$$a, b \sim v^2; \quad c, d, e, f, h \sim 1; \quad |t| \ll v. \tag{4}$$

Such a choice is motivated by the following considerations:

(i) The need to fulfill the electroweak symmetry breaking conditions,
(ii) To have $w \ll v$ sufficiently small, as required by the ρ-parameter constraint,
(iii) To keep doublet-triplet mixing low in general, and
(iv) To ensure that all quartic couplings are perturbative.

The mass terms for the singly charged scalars can be expressed in a compact form as

[1]For an analogous situation with two Higgs doublets, see for example [6].

$$\mathcal{L}_S^{\pm} = -(H^-, \phi^-)\mathcal{M}_+^2 \begin{pmatrix} H^+ \\ \phi^+ \end{pmatrix} \tag{5}$$

with

$$\mathcal{M}_+^2 = \begin{pmatrix} (q+h/2)v^2 & \sqrt{2}v(t^* - v_T h/2) \\ \sqrt{2}v(t - v_T^* h/2) & 2(q+h/2)w^2 \end{pmatrix} \quad \text{and}$$
$$q = \frac{|t|}{w}. \tag{6}$$

Keeping aside the charged Goldstone boson, the mass squared of the singly charged physical scalar is obtained as

$$m_{\Delta^+}^2 = \left(q + \frac{h}{2}\right)(v^2 + 2w^2), \tag{7}$$

while the doubly charged scalar mass is expressed as

$$m_{\Delta^{++}}^2 = (h+q)v^2 + 2fw^2. \tag{8}$$

Thus, in the limit $w \ll v$,

$$m_{\Delta^{++}}^2 - m_{\Delta^+}^2 \simeq \frac{h}{2}v^2. \tag{9}$$

Thus a substantial mass splitting between Δ^{++} and Δ^+ is in general difficult. This tends to disfavor the $\Delta^+ W^+$ decay channel of Δ^{++}, as compared to $\ell^+\ell^+$ and W^+W^+.

III. TWO-ZERO TEXTURE AND THE INADEQUACY OF A SINGLE TRIPLET

Strong evidence has accumulated in favor of neutrino oscillation from the solar, atmospheric, reactor and accelerator neutrino experiments over the past few years. It is now widely believed that neutrinos have nondegenerate masses and a very characteristic mixing pattern. A lot, however, is yet to be known, including the mass generation mechanism and the absolute values of the masses, as opposed to mass-squared differences which affect oscillation rates. Also, a lot of effort is on to ascertain the nature of neutrino mass hierarchy, including the signs of the mass-squared differences. A gateway to information of the above kinds is the light neutrino mass matrix, in a basis where the charged lepton mass matrix is diagonal.

Here, too, in the absence of very clear guidelines, various "textures" for the neutrino mass matrix are often investigated. A possibility that frequently enters into such investigations is one where the mass matrix has some zero entries, perhaps as the consequence of some built-in symmetry of lepton flavors. At the same time, such "zero textures" lead to a higher degree of predictiveness and interrelation between mass eigenvalues and mixing angles, by virtue of having fewer free paramaters (see for example [7]). In the context of Majorana neutrinos which have a symmetric mass matrix, various texture zeros have thus been studied from a number of angles. Of them, two-zero textures have a rather wide acceptability. It has been hinted in [8] that none of the seven possible two-zero-texture cases can be achieved by assuming only one scalar triplet.

To see this, note that there are seven possible two-zero textures for the 3×3 symmetric Majorana mass matrix of the light neutrinos, denoted by M_ν here. These are given by

$$\text{Case } A_1\text{: } M_\nu \sim \begin{pmatrix} 0 & 0 & \times \\ 0 & \times & \times \\ \times & \times & \times \end{pmatrix},$$
$$\text{Case } A_2\text{: } M_\nu \sim \begin{pmatrix} 0 & \times & 0 \\ \times & \times & \times \\ 0 & \times & \times \end{pmatrix}, \tag{10}$$
$$\text{Case } B_1\text{: } M_\nu \sim \begin{pmatrix} \times & \times & 0 \\ \times & 0 & \times \\ 0 & \times & \times \end{pmatrix},$$
$$\text{Case } B_2\text{: } M_\nu \sim \begin{pmatrix} \times & 0 & \times \\ 0 & \times & \times \\ \times & \times & 0 \end{pmatrix}, \tag{11}$$
$$\text{Case } B_3\text{: } M_\nu \sim \begin{pmatrix} \times & 0 & \times \\ 0 & 0 & \times \\ \times & \times & \times \end{pmatrix},$$
$$\text{Case } B_4\text{: } M_\nu \sim \begin{pmatrix} \times & \times & 0 \\ \times & \times & \times \\ 0 & \times & 0 \end{pmatrix}, \tag{12}$$
$$\text{Case } C\text{: } M_\nu \sim \begin{pmatrix} \times & \times & \times \\ \times & 0 & \times \\ \times & \times & 0 \end{pmatrix}. \tag{13}$$

These textures are defined in a basis where the charged lepton mass matrix is diagonal. In the context of Type-II seesaw the Yukawa couplings of scalar triplets Δ_k , which we write in 2×2 matrix notation, are given by

$$\mathcal{L}_Y = \frac{1}{2}\sum_{k=1}^{2} y_{ij}^{(k)} L_i^T C^{-1} i\tau_2 \Delta_k L_j + \text{H.c.}, \tag{14}$$

where $i, j = e, \mu, \tau$, C is the charge conjugation matrix, and the $y_{ij}^{(k)}$ are the symmetric Yukawa coupling matrices of the triplets Δ_k. From the above Lagrangian, the neutrino mass matrix is given by

$$\mathcal{M}_{ij}^{\nu} = w_k y_{ij}^k \tag{15}$$

with w_k being the VEV of the triplets. Among the neutrino mass terms, some are allowed, while others are not, as the consequence of a particular texture. This fact can be associated with a conserved global $U(1)$ summetry, under which all fields have some charge. Under this symmetry, the lepton doublets L_i and the scalar triplet Δ_k transform as

$$L_i \longrightarrow p_i L_i \quad \text{and} \quad \Delta_k \longrightarrow p_0 \Delta_k \tag{16}$$

with phase factors $|p_i|$, $|p_0| = 1$. An examination of each of the allowed textures reveals that the three phase factors for different lepton flavors, i.e. p_e, p_μ, p_τ, have to be different from each other. The Higgs doublet transforms trivially under the horizontal symmetry, thus enabling the charged-lepton mass matrix to be diagonal. Now, let us look at the consequence of such a synmetry when just one triplet is present. We shall see that this assumption leads us to a contradiction.

In all the seven possible two-texture-zero cases, the $\mu\tau$ element of $\mathcal{M}_\nu$ is nonzero. Thus, the corresponding Yukawa coupling element $y_{\mu\tau}$ must be nonzero, and the resulting interaction term must conserve the $U(1)$ charge. This implies

$$p_0 p_\mu p_\tau = 1. \tag{17}$$

We first examine the Cases B_1, B_2, B_3, B_4, and C. For these five cases, $y_{ee} \neq 0$. Therefore, upon applying the symmetry operation we have

$$p_0 p_e^2 = 1. \tag{18}$$

The inequality of the $U(1)$ charges for the different neutrino flavor eigenstates then results in $y_{e\mu}$ picking up a phase factor,

$$p_0 p_e p_\mu = \frac{p_\mu}{p_e} \neq 1. \tag{19}$$

This leads to the conclusion

$$y_{e\mu} = 0. \tag{20}$$

Proceeding in the same way with the $e\tau$ element of Yukawa coupling, we obtain

$$p_0 p_e p_\tau = \frac{p_\tau}{p_e} \neq 1, \tag{21}$$

which again implies

$$y_{e\tau} = 0. \tag{22}$$

On the other hand, we clearly see that in none of the cases B_1, B_2, B_3, B_4 and C, the Yukawa couplings $y_{e\mu}$ and $y_{e\tau}$ are both zero. Thus none of these five textures is viable when only one triplet is present in the scenario.

We next address the two remaining cases, namely A_1 and A_2. For both of these, one has $y_{\mu\mu} \neq 0$. Thus we have again after the symmetry operation

$$p_0 p_\mu^2 = 1. \tag{23}$$

However, that would again mean

$$p_0 p_\mu p_\tau = \frac{p_\tau}{p_\mu} \neq 1. \tag{24}$$

This in turn destroys the viability of these two textures as well. Thus one is forced to conclude that none of the seven possible two-zero-texture cases can be achieved by an Abelian horizontal symmetry assuming only one scalar triplet. But, when two or more triplets are present, then there will be more freedom in terms of the charges possessed by them, and the phase factor relations will be less constraining. Thus the contradictions that appear with a single triplet can be avoided, so that at least some of the seven possible two-zero textures are allowed. And therefore it is important to examine the phenomenological consequences of an augmented triplet sector, if the Type-II seesaw has to be consistent with two-zero textures. We proceed in that direction in the following sections.

IV. TWO SCALAR TRIPLETS AND A *CP*-VIOLATING PHASE

In view of the conclusions outlined in the previous section, one is thus encouraged to consider a scenario consisting of one complex doublet and two $Y = 2$ triplet scalars Δ_1, Δ_2, both written as 2×2 matrices,

$$\Delta_1 = \begin{pmatrix} \delta_1^+ & \sqrt{2}\delta_1^{++} \\ \sqrt{2}\delta_1^0 & -\delta_1^+ \end{pmatrix} \quad \text{and}$$
$$\Delta_2 = \begin{pmatrix} \delta_2^+ & \sqrt{2}\delta_2^{++} \\ \sqrt{2}\delta_2^0 & -\delta_2^+ \end{pmatrix}. \tag{25}$$

The VEVs of the scalar triplets are given by

$$\langle \Delta_1 \rangle_0 = \begin{pmatrix} 0 & 0 \\ w_1 & 0 \end{pmatrix} \quad \text{and}$$
$$\langle \Delta_2 \rangle_0 = \begin{pmatrix} 0 & 0 \\ w_2 & 0 \end{pmatrix}. \tag{26}$$

The VEV of the Higgs doublet is as usual given by Eq. (2).

The scalar potential in this model involving ϕ, Δ_1 and Δ_2 can be written as

$$V(\phi,\Delta_1,\Delta_2) = a\phi^\dagger\phi + \frac{1}{2}b_{kl}\mathrm{Tr}(\Delta_k^\dagger\Delta_l) + c(\phi^\dagger\phi)^2 + \frac{1}{4}d_{kl}(\mathrm{Tr}(\Delta_k^\dagger\Delta_l))^2 + \frac{1}{2}(e_{kl}-h_{kl})\phi^\dagger\phi\mathrm{Tr}(\Delta_k^\dagger\Delta_l) + \frac{1}{4}f_{kl}\mathrm{Tr}(\Delta_k^\dagger\Delta_l^\dagger)\mathrm{Tr}(\Delta_k\Delta_l) + h_{kl}\phi^\dagger\Delta_k^\dagger\Delta_l\phi + g\mathrm{Tr}(\Delta_1^\dagger\Delta_2)\mathrm{Tr}(\Delta_2^\dagger\Delta_1) + g'\mathrm{Tr}(\Delta_1^\dagger\Delta_1)\mathrm{Tr}(\Delta_2^\dagger\Delta_2) + (t_k\phi^\dagger\Delta_k\tilde{\phi} + \mathrm{H.c.}), \tag{27}$$

where summation over k, $l = 1, 2$ is understood. This potential is not the most general one, since we neglected some of the quartic terms. This is justified in view of the scope of this paper, as laid out in the Introduction.

In [4], all the VEVs as well as the parameters in the potential were assumed to be real. As has already been mentioned, this need not be the situation in general. To see the phenomenology including *CP*-violation, we make a minimal extension of the simplified scenario by postulating *one CP*-violating phase to exist. This entails a complex VEV for any one triplet (in our case we have chosen it to be Δ_1). At the same time, there is a complex phase in the coefficient t_1 of the trilinear term in the potential. Thus one can write $t_1 = |t_1|e^{i\beta}$ and $w_1 = |w_1|e^{i\alpha}$.

Using considerations very similar to those for the single-triplet model, we have taken

$$a, b_{kl} \sim v^2; \quad c, d_{kl}, e_{kl}, h_{kl}, f_{kl}, g, g' \sim 1; \quad |t_k| \ll v. \tag{28}$$

We have also chosen to restrict ourselves to cases where w_1, $w_2 \ll v$, keeping in mind the constraint on the ρ-parameter.

The mass eigenvalues, scalar mixing matrices, etc., following from the potential (27) can only be obtained numerically in general. However, one can use the smallness of the triplet VEVs w_k, and drop the quartic terms in the scalar triplets during the diagonalization of the mass matrices. This enables one to use approximate analytical expressions, which makes our broad conclusions somewhat transparent. However, the numerical results presented in Sec. V are obtained using the full potential (27), including the effects of the triplet VEVs.

It is convenient to speak in terms of the following matrices and vectors:

$$B = (b_{kl}), \qquad E = (e_{kl}), \qquad H = (h_{kl}), \tag{29}$$

$$t = \begin{pmatrix} |t_1|\cos\beta \\ t_2 \end{pmatrix}, \quad t' = \begin{pmatrix} |t_1|\sin\beta \\ 0 \end{pmatrix}, \quad w = \begin{pmatrix} |w_1|\cos\alpha \\ w_2 \end{pmatrix}, \quad w' = \begin{pmatrix} |w_1|\sin\alpha \\ 0 \end{pmatrix}. \tag{30}$$

In terms of them, the conditions for a stationary point of the potential are

$$\left(B + \frac{v^2}{2}(E-H)\right)w + v^2 t = 0, \tag{31}$$

$$a + cv^2 + \frac{1}{2}w^T(E-H)w + 2t\cdot w + 2t'\cdot w' + \frac{1}{2}w'^T(E-H)w' = 0, \tag{32}$$

$$\left(b_{11} + \frac{v^2}{2}(e_{11}-h_{11})\right)|w_1|\sin\alpha - v^2|t_1|\sin\beta = 0, \tag{33}$$

using the notation $t\cdot w = \sum_k t_k w_k$. These three equations are exact if one neglects all terms quartic in the triplet VEVs in $V_0 \equiv V(\langle\phi\rangle_0, \langle\Delta\rangle_0)$. In Eq. (32) we have already divided by v, assuming $v \neq 0$. The small VEVs w_k are thereafter obtained as

$$w = -v^2\left(B + \frac{1}{2}v^2(E-H)\right)^{-1}t. \tag{34}$$

And from Eq. (33) the phase of t_1 can be expressed as

$$\sin\beta = \frac{v^{-2}(b_{11} + \frac{v^2}{2}(e_{11}-h_{11}))|w_1|\sin\alpha}{|t_1|}. \tag{35}$$

This reiterates the fact that the phases t_1 and w_1 are related to each other. It is also evident from (35) that the value of the angle α has to be $n\pi$ where $n = 0, 1, 2, 3, \ldots$. when the phase β is absent.

We next discuss the mass matrices of charged scalars. The mass matrix of the doubly charged scalars is obtained as

$$\mathcal{M}^2_{++} = B + \frac{v^2}{2}(E+H). \tag{36}$$

It is interesting to note that if we drop those quartic terms for simplification from our scalar potential, then our doubly charged mass matrix remains the same as in [4]. This gives the impression that the relative phase between triplets does not affect the doubly charged mass matrix if we drop the quartic terms in the potential. But in our numerical calculation, where we have taken the full scalar potential including the quartic terms, we find such a dependence, arising obviously from the quartic terms. This will be discussed further in the next section.

As for the singly charged fields Δ_k^+, one has to consider their mixing with ϕ^+ of the Higgs doublet. This introduces the CP-violating phase into the singly charged mass matrix. We write the mass term as

$$-\mathcal{L}_S^{\pm} = (\delta_1^-, \delta_2^-, \phi^-)\mathcal{M}_+^2 \begin{pmatrix} \delta_1^+ \\ \delta_2^+ \\ \phi^+ \end{pmatrix} + \text{H.c.}, \tag{37}$$

and Eq. (27) leads to

$$\mathcal{M}_+^2 = \begin{pmatrix} B + \frac{v^2}{2}E & \sqrt{2}v(t - Hw/2) \\ \sqrt{2}v(t - Hw/2)^\dagger & a + cv^2 + \frac{1}{2}w^T(E+H)w + \frac{1}{2}w'^T(E+H)w' \end{pmatrix}. \tag{38}$$

Now, this mass matrix must have a zero eigenvalue, corresponding to the would-be-Goldstone boson. Indeed, on substituting the minimization equations (31), (32) and (33), we see that

$$\text{Det}(\mathcal{M}_+^2) = 0, \tag{39}$$

which ensures a consistency check.

The mass matrices (37) and (38) are diagonalized by

$$\begin{aligned} U_1^\dagger \mathcal{M}_{++}^2 U_1 &= \text{diag}(M_1^2, M_2^2) \quad \text{and} \\ U_2^\dagger \mathcal{M}_+^2 U_2 &= \text{diag}(\mu_1^2, \mu_2^2, 0), \end{aligned} \tag{40}$$

respectively, with

$$\begin{aligned} \begin{pmatrix} \delta_1^{++} \\ \delta_2^{++} \end{pmatrix} &= U_1 \begin{pmatrix} H_1^{++} \\ H_2^{++} \end{pmatrix}, \\ \begin{pmatrix} \delta_1^{+} \\ \delta_2^{+} \\ \phi^{+} \end{pmatrix} &= U_2 \begin{pmatrix} H_1^{+} \\ H_2^{+} \\ G^{+} \end{pmatrix}. \end{aligned} \tag{41}$$

We have denoted the fields with definite mass by H_k^{++} and H_k^+, and G^+ is the charged would-be-Goldstone boson.

We also outline the neutral sector of the model, which cannot now be separated into CP-even and CP-odd sectors. Thus the mass matrix for the neutral sector of the present scenario turns out to be a 6×6 matrix, including mixing between real and imaginary parts of the complex neutral fields. The symmetric neutral mass matrix is denoted by $\mathcal{M}_{\text{neut}}$, whose elements are listed in the Appendix. So, the mass term for the neutral part can be written as

$$-\mathcal{L}_S^0 = (N_{01}, N_{02}, N_{03}, N_{04}, N_{05}, N_{06})\mathcal{M}_{\text{neut}}^2 \begin{pmatrix} N_{01} \\ N_{02} \\ N_{03} \\ N_{04} \\ N_{05} \\ N_{06} \end{pmatrix} + \text{H.c.}, \tag{42}$$

where N_{0n} are the neutral states in the flavor basis. This mass matrix is diagonalized by

$$U_3^\dagger \mathcal{M}_{\text{neut}}^2 U_3 = \text{diag}(M_{01}^2, M_{02}^2, M_{03}^2, M_{04}^2, M_h^2, 0) \tag{43}$$

with

$$\begin{pmatrix} N_{01} \\ N_{02} \\ N_{03} \\ N_{04} \\ N_{05} \\ N_{06} \end{pmatrix} = U_3 \begin{pmatrix} H_{01} \\ H_{02} \\ H_{03} \\ H_{04} \\ h \\ G_0 \end{pmatrix}, \tag{44}$$

where h is identified with the Standard Model Higgs boson and G_0 is the neutral Goldstone boson.

It is interesting to note that once we remove the phases of the coefficient of the trilinear term in scalar potential and the VEV of triplet H_1^{++} by setting $\alpha = \beta = 0$, then the mixing between the CP-even and CP-odd scalars vanishes and we get back the usual separate 3×3 matrices for these two sectors. This also serves as a consistency check for the model. And of course the lightest neutral scalar of this sector can be identified with SM Higgs.

The $\Delta L = 2$ Yukawa interactions of the triplets are

$$\mathcal{L}_Y = \frac{1}{2}\sum_{k=1}^{2} y_{ij}^{(k)} L_i^T C^{-1} i\tau_2 \Delta_k L_j + \text{H.c.}, \tag{45}$$

where C is the charge conjugation matrix, the $y_{ij}^{(k)}$ are the symmetric Yukawa coupling matrices of the triplets Δ_k, and the i, j are the summation indices over the three neutrino flavors. The charged-lepton mass matrix is diagonal in this basis.

The neutrino mass matrix is generated from $\mathcal{L}_Y$ as

$$(M_\nu)_{ij} = y_{ij}^{(1)}|w_1|\cos\alpha + y_{ij}^{(2)}w_2. \tag{46}$$

This relates the Yukawa coupling constants $y_{ij}^{(1)}$, $y_{ij}^{(2)}$ and the real part of the triplet VEVs, namely, $|w_1|\cos\alpha$ and w_2.

The neutrino mass eigenvalues are fixed according to a particular type of mass spectrum. In this work we illustrate our points, without any loss of generality, in the context of the normal hierarchy, setting the lowest neutrino mass eigenvalue to zero. Next, using the observed central values of the various lepton mixing angles, the elements of the neutrino mass matrix M_ν can be found by using

$$M_\nu = U^\dagger \hat{M}_\nu U, \tag{47}$$

where U is the Pontecorvo-Maki-Nakagawa-Sakata matrix given by [9]

$$U = \begin{pmatrix} c_{12}c_{13} & s_{12}c_{13} & s_{13}e^{-i\delta} \\ -s_{12}c_{23} - c_{12}s_{23}s_{13}e^{i\delta} & c_{12}c_{23} - s_{12}s_{23}s_{13}e^{i\delta} & s_{23}c_{13} \\ s_{12}s_{23} - c_{12}c_{23}s_{13}e^{i\delta} & -c_{12}s_{23} - s_{12}c_{23}s_{13}e^{i\delta} & c_{23}c_{13} \end{pmatrix} \tag{48}$$

and $\hat{M}_\nu$ is the diagonal matrix of the neutrino masses. We have neglected possible Majorana phases, and the recent global analysis of neutrino data is used to compute the elements of U [10]. Also, the phase δ has been set to zero. For θ_{13}, the results from the Daya Bay and RENO experiments [11,12] have been used.

After all this, all terms of the left-hand side of Eq. (45) are approximately known, which is sufficient for predicting phenomenology in the 100 GeV–1 TeV scale. The actual mass matrix thus constructed, on numerical evaluation, approximately reflects a two-zero texture which is one of the motivations of this study.

For each benchmark point used in the next section, w_1 and w_2 get determined by values of the other parameters in the scalar potential. Of course, the coupling matrices $y^{(1)}$ and $y^{(2)}$ are still indeterminate. We fix the matrix $y^{(2)}$ by choosing a single suitable value for all elements of the μ-τ block and a smaller value for the rest of the matrix. As has already been mentioned in [4], our broad conclusions do not depend on this "working rule."

Of course, the success of a two-triplet scenario in the context of a seesaw mechanism requires the electroweak vacuum to be (meta)stable till at least the seesaw scale. In general, the tendency of the top quark Yukawa coupling to turn the doublet quartic couplings negative is responsible for the loss of stability. Additional scalar quartic couplings usually offset this effect [13], and the present scenario is no exception. It been shown in [14] that one can ensure stability up to $10^{16\text{–}18}$ GeV with a single triplet. With the low-energy quartic couplings not too different from these, and with one more triplet, interacting with the doublet, introduced, the situation is even more optimistic. Moreover, the acceptence of a metastable electroweak vacuum can help the scenario even further.

TABLE I. Charged scalar masses for phase $\alpha = 30°$.

$\alpha = 30°$	Mass [GeV]	BP 1	BP 2	BP 3	BP 4
Scenario 1	H_1^{++}	516.61	513.83	522.13	537.62
	H_2^{++}	391.40	389.82	426.93	440.96
	H_1^{+}	516.58	513.81	522.10	537.55
	H_2^{+}	390.60	389.79	408.83	416.30
Scenario 2	H_1^{++}	526.00	529.85	477.38	485.76
	H_2^{++}	397.61	390.10	389.10	389.33
	H_1^{+}	525.94	529.80	477.34	485.70
	H_2^{+}	393.79	390.01	389.00	389.28
Scenario 3	H_1^{++}	558.71	562.35	485.76	477.38
	H_2^{++}	427.00	407.20	389.33	389.10
	H_1^{+}	557.59	559.11	485.70	477.34
	H_2^{+}	392.90	405.91	389.28	389.00

TABLE II. Neutral scalar masses for phase $\alpha = 30°$.

$\alpha = 30°$	Mass [GeV]	BP 1	BP 2	BP 3	BP 4
Scenario 1	H_{01}	730.57	726.65	738.36	760.19
	H_{02}	730.49	726.62	738.32	760.15
	H_{03}	552.30	551.25	551.40	552.65
	H_{04}	552.15	551.20	551.34	552.56
	h	125.16	125.18	125.20	125.15
Scenario 2	H_{01}	743.85	749.33	675.11	686.96
	H_{02}	743.00	749.25	675.00	686.90
	H_{03}	552.21	551.50	550.17	550.53
	H_{04}	552.10	551.39	550.05	550.40
	h	125.21	125.18	125.22	125.23
Scenario 3	H_{01}	787.10	789.25	687.00	676.15
	H_{02}	787.00	789.10	686.90	676.08
	H_{03}	541.16	542.00	552.21	549.90
	H_{04}	541.07	541.91	552.00	549.75
	h	125.23	125.26	125.13	125.16

TABLE III. Decay branching ratios and production cross sections for doubly charged scalars for phase $\alpha = 30°$.

$\alpha = 30°$	Data	BP 1	BP 2	BP 3	BP 4
	$\mathrm{BR}(H_1^{++} \to H_2^{++} h)$	5.1×10^{-3}	Not allowed	Not allowed	Not allowed
	$\mathrm{BR}(H_1^{++} \to H_2^{+} W^{+})$	0.99	0.99	0.79	0.99
	$\mathrm{BR}(H_1^{++} \to W^{+} W^{+})$	2.8×10^{-3}	6.5×10^{-2}	0.21	3.1×10^{-7}
	$\mathrm{BR}(H_1^{++} \to \ell_i^{+} \ell_j^{+})$	4.8×10^{-21}	1.6×10^{-20}	1.3×10^{-18}	2.1×10^{-23}
Scenario 1	$\mathrm{BR}(H_2^{++} \to W^{+} W^{+})$	0.99	0.99	0.99	0.99
	$\mathrm{BR}(H_2^{++} \to \ell_i^{+} \ell_j^{+})$	1.6×10^{-18}	2.7×10^{-18}	3.9×10^{-17}	1.3×10^{-20}
	$\sigma(pp \to H_1^{++} H_1^{--})$	1.10 fb	1.13 fb	1.05 fb	0.42 fb
	$\sigma(pp \to H_2^{++} H_2^{--})$	3.97 fb	4.10 fb	2.70 fb	1.06 fb
	$\mathrm{BR}(H_1^{++} \to H_2^{++} h)$	0.84	0.96	Not allowed	Not allowed
	$\mathrm{BR}(H_1^{++} \to H_2^{+} W^{+})$	0.13	0.03	0.76	0.42
	$\mathrm{BR}(H_1^{++} \to W^{+} W^{+})$	3.1×10^{-20}	1.9×10^{-20}	1.2×10^{-19}	2.8×10^{-21}
	$\mathrm{BR}(H_1^{++} \to \ell_i^{+} \ell_j^{+})$	0.03	8.9×10^{-3}	0.24	0.58
Scenario 2	$\mathrm{BR}(H_2^{++} \to W^{+} W^{+})$	1.9×10^{-19}	2.8×10^{-19}	1.8×10^{-20}	3.7×10^{-19}
	$\mathrm{BR}(H_2^{++} \to \ell_i^{+} \ell_j^{+})$	0.99	0.99	0.99	0.99
	$\sigma(pp \to H_1^{++} H_1^{--})$	1.01 fb	1.02 fb	1.56 fb	1.43 fb
	$\sigma(pp \to H_2^{++} H_2^{--})$	3.60 fb	4.04 fb	3.97 fb	3.95 fb
	$\mathrm{BR}(H_1^{++} \to H_2^{++} h)$	0.99	0.99	Not allowed	Not allowed
	$\mathrm{BR}(H_1^{++} \to H_2^{+} W^{+})$	2.1×10^{-3}	1.3×10^{-2}	0.99	0.99
	$\mathrm{BR}(H_1^{++} \to W^{+} W^{+})$	2.6×10^{-14}	3.1×10^{-14}	4.3×10^{-10}	2.8×10^{-11}
	$\mathrm{BR}(H_1^{++} \to \ell_i^{+} \ell_j^{+})$	1.5×10^{-11}	2.3×10^{-11}	3.7×10^{-7}	5.4×10^{-8}
Scenario 3	$\mathrm{BR}(H_2^{++} \to W^{+} W^{+})$	0.03	0.01	0.04	0.02
	$\mathrm{BR}(H_2^{++} \to \ell_i^{+} \ell_j^{+})$	0.97	0.99	0.96	0.98
	$\sigma(pp \to H_1^{++} H_1^{--})$	0.77 fb	0.74 fb	1.45 fb	1.58 fb
	$\sigma(pp \to H_2^{++} H_2^{--})$	3.61 fb	2.75 fb	3.95 fb	3.98 fb

V. BENCHMARK POINTS AND NUMERICAL PREDICTIONS

The trademark signal of Higgs triplets is contained in the doubly charged components. In the current scenario, too, one would like to see the signatures of the two doubly charged scalars, especially the heavier one, namely H_1^{++} whose decays have already been shown to contain a rather rich phenomenology.

The H_1^{++}, produced at the LHC via the Drell-Yan process, can in general have two-body decays in the following channels:

TABLE IV. Charged scalar masses for phase $\alpha = 45°$.

$\alpha = 45°$	Mass [GeV]	BP 1	BP 2	BP 3	BP 4
	H_1^{++}	542.27	539.35	549.85	566.55
Scenario 1	H_2^{++}	406.60	405.20	438.46	450.96
	H_1^{+}	542.22	539.20	548.73	564.92
	H_2^{+}	405.90	405.07	422.28	428.94
	H_1^{++}	543.30	538.15	551.62	564.34
Scenario 2	H_2^{++}	405.10	404.10	440.10	448.82
	H_1^{+}	542.50	537.65	550.90	563.65
	H_2^{+}	405.00	403.20	439.72	447.90
	H_1^{++}	545.82	540.32	550.90	567.80
Scenario 3	H_2^{++}	409.80	405.00	439.50	452.45
	H_1^{+}	544.71	539.46	550.15	565.90
	H_2^{+}	409.00	404.75	425.38	432.80

TABLE V. Neutral scalar masses for phase $\alpha = 45°$.

$\alpha = 45°$	Mass [GeV]	BP 1	BP 2	BP 3	BP 4
	H_{01}	766.78	762.75	774.79	797.22
Scenario 1	H_{02}	766.60	762.11	774.23	797.00
	H_{03}	573.00	572.50	575.50	576.17
	H_{04}	572.65	572.00	575.15	575.95
	h	125.15	125.22	125.19	125.13
	H_{01}	768.10	760.37	772.90	795.85
Scenario 2	H_{02}	768.00	760.13	772.75	795.50
	H_{03}	575.32	570.00	574.30	576.85
	H_{04}	575.15	569.22	573.78	576.20
	h	125.12	125.16	125.24	125.17
	H_{01}	771.10	758.52	778.10	798.37
Scenario 3	H_{02}	770.85	758.00	777.85	798.00
	H_{03}	577.31	568.75	578.29	577.21
	H_{04}	577.00	568.13	578.00	577.00
	h	125.18	125.21	125.13	125.16

TABLE VI. Decay branching ratios and production cross sections for doubly charged scalars for phase $\alpha = 45°$.

$\alpha = 45°$	Data	BP 1	BP 2	BP 3	BP 4
Scenario 1	$\mathrm{BR}(H_1^{++} \to H_2^{++}h)$	0.99	0.99	Not allowed	Not allowed
	$\mathrm{BR}(H_1^{++} \to H_2^{+}W^{+})$	8.2×10^{-4}	9.1×10^{-4}	0.90	0.96
	$\mathrm{BR}(H_1^{++} \to W^{+}W^{+})$	2.4×10^{-5}	1.7×10^{-4}	0.09	0.04
	$\mathrm{BR}(H_1^{++} \to \ell_i^{+}\ell_j^{+})$	3.1×10^{-22}	3.8×10^{-22}	6.1×10^{-19}	4.2×10^{-20}
	$\mathrm{BR}(H_2^{++} \to W^{+}W^{+})$	0.99	0.99	0.99	0.99
	$\mathrm{BR}(H_2^{++} \to \ell_i^{+}\ell_j^{+})$	7.4×10^{-19}	8.3×10^{-19}	2.1×10^{-19}	6.7×10^{-19}
	$\sigma(pp \to H_1^{++}H_1^{--})$	0.88 fb	0.87 fb	0.80 fb	0.71 fb
	$\sigma(pp \to H_2^{++}H_2^{--})$	3.39 fb	3.33 fb	2.43 fb	2.13 fb
Scenario 2	$\mathrm{BR}(H_1^{++} \to H_2^{++}h)$	0.99	0.99	Not allowed	Not allowed
	$\mathrm{BR}(H_1^{++} \to H_2^{+}W^{+})$	4.5×10^{-4}	3.9×10^{-4}	0.64	0.88
	$\mathrm{BR}(H_1^{++} \to W^{+}W^{+})$	1.3×10^{-21}	9.1×10^{-22}	7.6×10^{-20}	6.4×10^{-21}
	$\mathrm{BR}(H_1^{++} \to \ell_i^{+}\ell_j^{+})$	3.1×10^{-6}	1.7×10^{-4}	0.36	0.12
	$\mathrm{BR}(H_2^{++} \to W^{+}W^{+})$	2.7×10^{-20}	2.5×10^{-19}	3.2×10^{-19}	5.7×10^{-20}
	$\mathrm{BR}(H_2^{++} \to \ell_i^{+}\ell_j^{+})$	0.99	0.99	0.99	0.99
	$\sigma(pp \to H_1^{++}H_1^{--})$	0.93 fb	0.89 fb	0.86 fb	0.75 fb
	$\sigma(pp \to H_2^{++}H_2^{--})$	2.55 fb	3.35 fb	2.46 fb	2.18 fb
Scenario 3	$\mathrm{BR}(H_1^{++} \to H_2^{++}h)$	0.99	0.99	Not allowed	Not allowed
	$\mathrm{BR}(H_1^{++} \to H_2^{+}W^{+})$	3.6×10^{-5}	1.4×10^{-4}	0.99	0.99
	$\mathrm{BR}(H_1^{++} \to W^{+}W^{+})$	8.6×10^{-14}	7.3×10^{-13}	1.4×10^{-9}	5.8×10^{-10}
	$\mathrm{BR}(H_1^{++} \to \ell_i^{+}\ell_j^{+})$	4.8×10^{-11}	3.7×10^{-11}	5.6×10^{-11}	4.7×10^{-9}
	$\mathrm{BR}(H_2^{++} \to W^{+}W^{+})$	0.02	0.04	0.97	0.05
	$\mathrm{BR}(H_2^{++} \to \ell_i^{+}\ell_j^{+})$	0.98	0.96	0.03	0.95
	$\sigma(pp \to H_1^{++}H_1^{--})$	0.92 fb	0.95 fb	0.84 fb	0.73 fb
	$\sigma(pp \to H_2^{++}H_2^{--})$	3.42 fb	3.37 fb	2.44 fb	2.15 fb

$$H_1^{++} \to H_2^{++}h, \tag{49}$$

$$H_1^{++} \to \ell_i^{+}\ell_j^{+}, \tag{50}$$

$$H_1^{++} \to W^{+}W^{+}, \tag{51}$$

$$H_1^{++} \to H_2^{+}W^{+}, \tag{52}$$

$$H_2^{++} \to \ell_i^{+}\ell_j^{+}, \tag{53}$$

$$H_2^{++} \to W^{+}W^{+}, \tag{54}$$

where h is the SM-like Higgs and ℓ_i, $\ell_j = e$, μ.

The decay modes (49) and (52) are absent in the single-triplet model. On the other hand, mixing between two

TABLE VII. Charged scalar masses for phase $\alpha = 60°$.

$\alpha = 60°$	Mass [GeV]	BP 1	BP 2	BP 3	BP 4
Scenario 1	H_1^{++}	557.90	563.51	564.20	556.56
	H_2^{++}	412.20	411.51	434.37	439.71
	H_1^{+}	557.62	563.25	559.18	548.00
	H_2^{+}	411.65	411.18	423.27	426.15
Scenario 2	H_1^{++}	558.20	565.20	566.40	554.30
	H_2^{++}	411.90	413.61	436.56	438.12
	H_1^{+}	558.00	564.50	565.90	553.65
	H_2^{+}	410.75	412.85	435.85	435.32
Scenario 3	H_1^{++}	556.65	560.30	567.80	552.90
	H_2^{++}	410.25	408.35	437.90	436.59
	H_1^{+}	556.00	559.75	563.21	550.00
	H_2^{+}	409.85	407.80	425.56	429.11

TABLE VIII. Neutral scalar masses for phase $\alpha = 60°$.

$\alpha = 60°$	Mass [GeV]	BP 1	BP 2	BP 3	BP 4
Scenario 1	H_{01}	788.52	796.91	784.64	765.05
	H_{02}	788.35	796.27	784.21	764.62
	H_{03}	581.43	583.16	579.62	577.78
	H_{04}	581.32	582.95	579.13	577.21
	h	125.16	125.24	125.14	125.20
Scenario 2	H_{01}	790.21	793.82	786.52	762.90
	H_{02}	790.00	793.11	786.09	762.42
	H_{03}	579.32	580.16	582.32	574.21
	H_{04}	579.00	579.92	582.00	573.86
	h	125.15	125.10	125.21	125.09
Scenario 3	H_{01}	786.51	790.63	785.00	760.71
	H_{02}	786.00	790.27	784.32	760.29
	H_{03}	577.82	576.21	580.14	570.90
	H_{04}	577.50	576.00	579.55	570.58
	h	125.23	125.14	125.23	125.18

TABLE IX. Decay branching ratios and production cross sections for doubly charged scalars for phase $\alpha = 60°$.

$\alpha = 60°$	Data	BP 1	BP 2	BP 3	BP 4
Scenario 1	$\mathrm{BR}(H_1^{++} \to H_2^{++} h)$	0.99	0.98	0.99	Not allowed
	$\mathrm{BR}(H_1^{++} \to H_2^{+} W^{+})$	3.9×10^{-4}	2.6×10^{-2}	0.01	0.94
	$\mathrm{BR}(H_1^{++} \to W^{+} W^{+})$	1.7×10^{-5}	8.9×10^{-3}	6.9×10^{-5}	0.05
	$\mathrm{BR}(H_1^{++} \to \ell_i^{+} \ell_j^{+})$	2.6×10^{-22}	4.7×10^{-21}	3.1×10^{-22}	5.6×10^{-20}
	$\mathrm{BR}(H_2^{++} \to W^{+} W^{+})$	0.99	0.99	0.99	0.99
	$\mathrm{BR}(H_2^{++} \to \ell_i^{+} \ell_j^{+})$	6.7×10^{-19}	7.2×10^{-19}	5.3×10^{-20}	3.5×10^{-15}
	$\sigma(pp \to H_1^{++} H_1^{--})$	0.79 fb	0.71 fb	0.72 fb	0.84 fb
	$\sigma(pp \to H_2^{++} H_2^{--})$	3.22 fb	3.15 fb	2.48 fb	2.51 fb
Scenario 2	$\mathrm{BR}(H_1^{++} \to H_2^{++} h)$	0.99	0.79	0.99	Not allowed
	$\mathrm{BR}(H_1^{++} \to H_2^{+} W^{+})$	3.2×10^{-5}	0.21	3.1×10^{-3}	0.88
	$\mathrm{BR}(H_1^{++} \to W^{+} W^{+})$	3.9×10^{-22}	5.6×10^{-22}	5.9×10^{-22}	4.3×10^{-22}
	$\mathrm{BR}(H_1^{++} \to \ell_i^{+} \ell_j^{+})$	2.1×10^{-4}	1.4×10^{-4}	3.7×10^{-4}	0.12
	$\mathrm{BR}(H_2^{++} \to W^{+} W^{+})$	3.2×10^{-19}	5.6×10^{-20}	7.8×10^{-18}	6.3×10^{-19}
	$\mathrm{BR}(H_2^{++} \to \ell_i^{+} \ell_j^{+})$	0.99	0.99	0.99	0.99
	$\sigma(pp \to H_1^{++} H_1^{--})$	0.77 fb	0.74 fb	0.81 fb	0.86 fb
	$\sigma(pp \to H_2^{++} H_2^{--})$	3.26 fb	3.19 fb	2.46 fb	2.53 fb
Scenario 3	$\mathrm{BR}(H_1^{++} \to H_2^{++} h)$	0.99	0.90	0.99	Not allowed
	$\mathrm{BR}(H_1^{++} \to H_2^{+} W^{+})$	2.5×10^{-4}	0.10	1.2×10^{-2}	0.99
	$\mathrm{BR}(H_1^{++} \to W^{+} W^{+})$	9.3×10^{-15}	2.7×10^{-14}	5.3×10^{-11}	5.1×10^{-11}
	$\mathrm{BR}(H_1^{++} \to \ell_i^{+} \ell_j^{+})$	6.4×10^{-11}	1.7×10^{-12}	7.6×10^{-13}	2.3×10^{-9}
	$\mathrm{BR}(H_2^{++} \to W^{+} W^{+})$	0.03	0.04	0.89	0.02
	$\mathrm{BR}(H_2^{++} \to \ell_i^{+} \ell_j^{+})$	0.97	0.96	0.11	0.98
	$\sigma(pp \to H_1^{++} H_1^{--})$	0.81 fb	0.75 fb	0.72 fb	0.83 fb
	$\sigma(pp \to H_2^{++} H_2^{--})$	3.28 fb	3.20 fb	2.50 fb	2.54 fb

triplets opens up situations where the mass separation between H_1^{++}, H_2^{++} and H_1^{++}, H_2^{+} is sufficient to kinematically allow the transitions (49) and (52). The decay (49) opens up a spectacular signal, especially when H_2^{++} mostly decays into two same sign leptons, leading to

$$H_1^{++} \to \ell_i^{+} \ell_j^{+} h. \tag{55}$$

Let us denote the mass of SM Higgs by M_h, that of H_k^{++} by M_k and that of H_k^{+} by μ_k ($k = 1, 2$). Then, in the convention $M_1 > M_2$, $\mu_1 > \mu_2$, the decays (49) and (52) are possible only if $M_1 > M_2 + M_h$ and $M_1 > \mu_2 + m_W$. We demonstrate numerically that this can naturally happen, by considering three distinct regions of the parameter space and selecting four BPs for each region. The relative phase between two triplets also plays an important roll in these

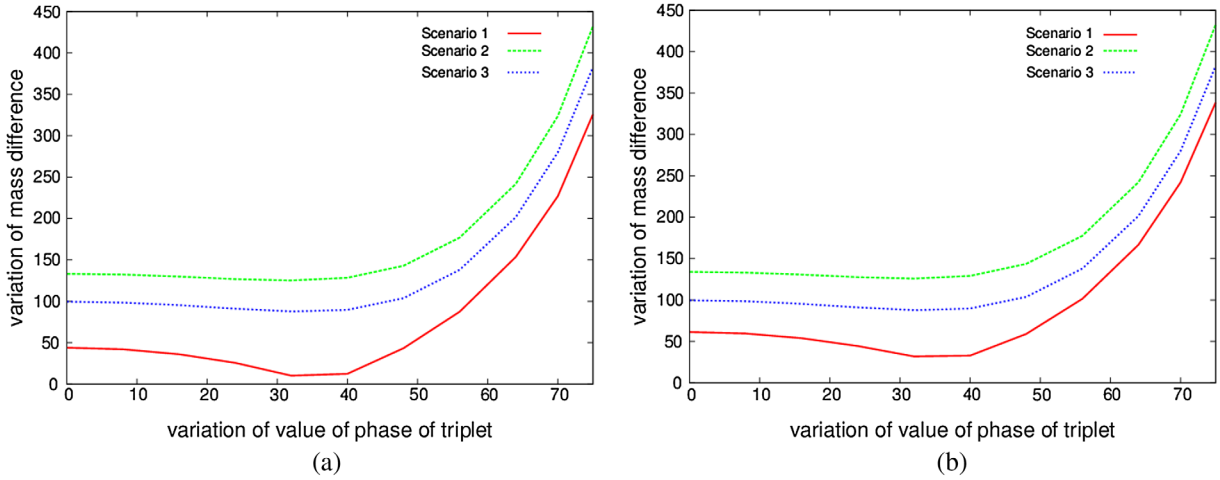

FIG. 1. Variation of mass difference between (a) $\mathcal{H}_1^{++}$ and $\mathcal{H}_2^{++}$ and (b) $\mathcal{H}_1^{++}$ and $\mathcal{H}_2^{+}$ with phase of triplet α.

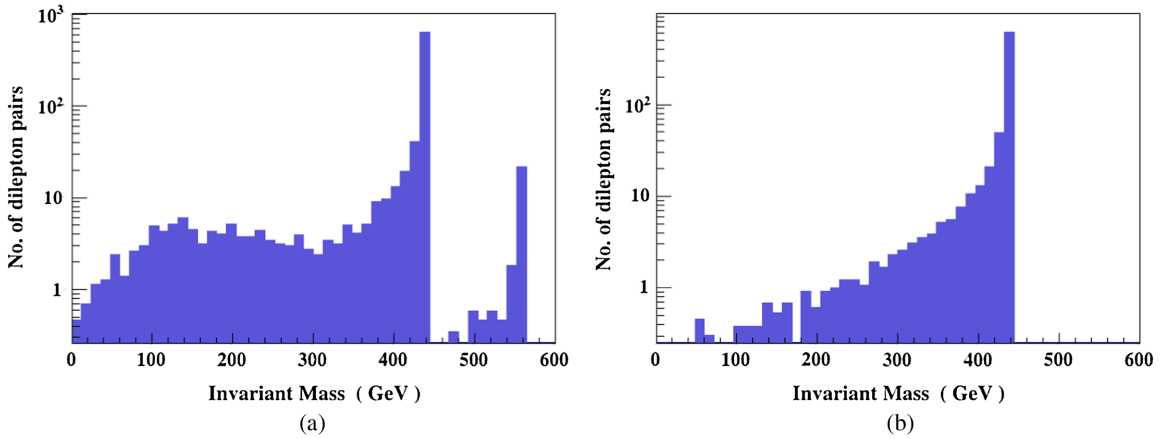

FIG. 2. Invariant mass distribution of same sign dileptons for (a) $\alpha = 60°$ and (b) $\alpha = 65°$ for BP 4 of Scenario 2.

cases. In order to emphasize this, we have also chosen three different values of the phase, namely $\alpha = 30°$, 45° and 60° for each benchmark point. Thus we have considered 36 BPs altogether, comprising three distinct regions of the parameter space and relative phases between triplets to justify our findings.

We have seen that, in a single-triplet model, the doubly charged Higgs decays into either $\ell_i^+\ell_j^+$ or W^+W^+. The former is controlled by the $\Delta L = 2$ Yukawa couplings y_{ij}, while the latter is driven by w, the triplet VEV. Neutrino masses are given by (46), implying large values of y_{ij} for small w, and vice versa. Interestingly, the presence of a triplet phase through the $\cos\alpha$ term in this equation actually suppresses the VEV w_1 of the first triplet. This in turn implies that we get higher values for Yukawa coupling matrix entries y_1^{ij} compared to the case where *CP*-violating effects are absent. Accordingly, we have identified, for the chosen values of the triplet phase, three regions in the parameter space, corresponding to

(i) $\Gamma(H_{1,2}^{++} \to \ell_i^+\ell_j^+) \ll \Gamma(H_{1,2}^{++} \to W^+W^+)$,
(ii) $\Gamma(H_{1,2}^{++} \to \ell_i^+\ell_j^+) \gg \Gamma(H_{1,2}^{++} \to W^+W^+)$,
(iii) $\Gamma(H_{1,2}^{++} \to \ell_i^+\ell_j^+) \sim \Gamma(H_{1,2}^{++} \to W^+W^+)$.

These are referred to as scenarios 1, 2 and 3, respectively, in the subsequent discussion.

The masses of the various physical scalars and some of their phenomenological properties are shown in Tables I–IX. Although our study involves mainly the phenomenology of charged scalars, we have also listed the masses of neutral scalars. It should be noted that the lightest neutral scalar, dominated by the doublet component, has mass ∼125 GeV for each BP, identifying it with the observed Higgs particle.

In Ref. [4], we had concentrated on those benchmark points in the parameter space, for which $H_1^{++} \to H_2^+W^+$ becomes a dominant decay mode. Here we draw the reader's attention to an interesting complementary situation: one can have, in certain regions of the parameter space, $H_1^{++} \to H_2^{++}h$ as the dominant channel in H_1^{++} decay. Since the triplet masses are free parameters, this can of course happen without any "theoretical design." However, the presence of the *CP*-violating phase can also play an interesting role here. This is demonstrated in Fig. 1. To understand the situation, suppose the mass parameters in the potential are fixed in such a way that the decay $H_1^{++} \to H_2^{++}h$ is not possible for $\alpha = 0$. Now, if the *CP*-violating phase α is gradually increased from zero, keeping all the other parameters fixed, then both the mass differences $m_{H_1^{++}} - m_{H_2^{++}}$ and $m_{H_1^{++}} - m_{H_2^+}$ start increasing rather sharply for $\alpha \gtrsim 60°$. This is because the degree of doublet-triplet mixing for Δ_1 in our parametrization changes with α. In such situations, as shown, for example, in Table IX, the quartic couplings cause the decay $H_1^{++} \to H_2^{++}h$ to dominate over $H_1^{++} \to H_2^+W^+$. Thus, other than the free parameters corresponding to the scalar masses, the *CP*-violating phase has a part to play in the phenomenology of a two-triplet scenario. One consequence of this will be discussed below.

Earlier, we neglected contributions from the quartic terms in our scalar potential in the approximate forms of the doubly and singly charged mass matrices. However, the import of the phase is not properly captured unless one retains these terms. Thus it is only via a full numerical analysis of the potential retaining all terms that the above effect of the phase of the trilinear term becomes apparent.

It should also be noted that the cosine of the complex phase suppresses the contribution to neutrino masses. Consequently, for the same triplet VEV, one requires larger values of the Yukawa interaction strengths. This makes the l^+l^+ decay mode of a doubly charged scalar more competitive with W^+W^+, as compared to the results in [4].

The branching ratios for a given scalar in different channels are of course dependent on the various parameters that characterize a BP. We list all the charged scalar masses in Tables I, IV and VII. Moreover, the neutral scalar masses are shown in Tables II, V and VIII for three different values of triplet phase α. The branching ratios for H_1^{++} and H_2^{++}

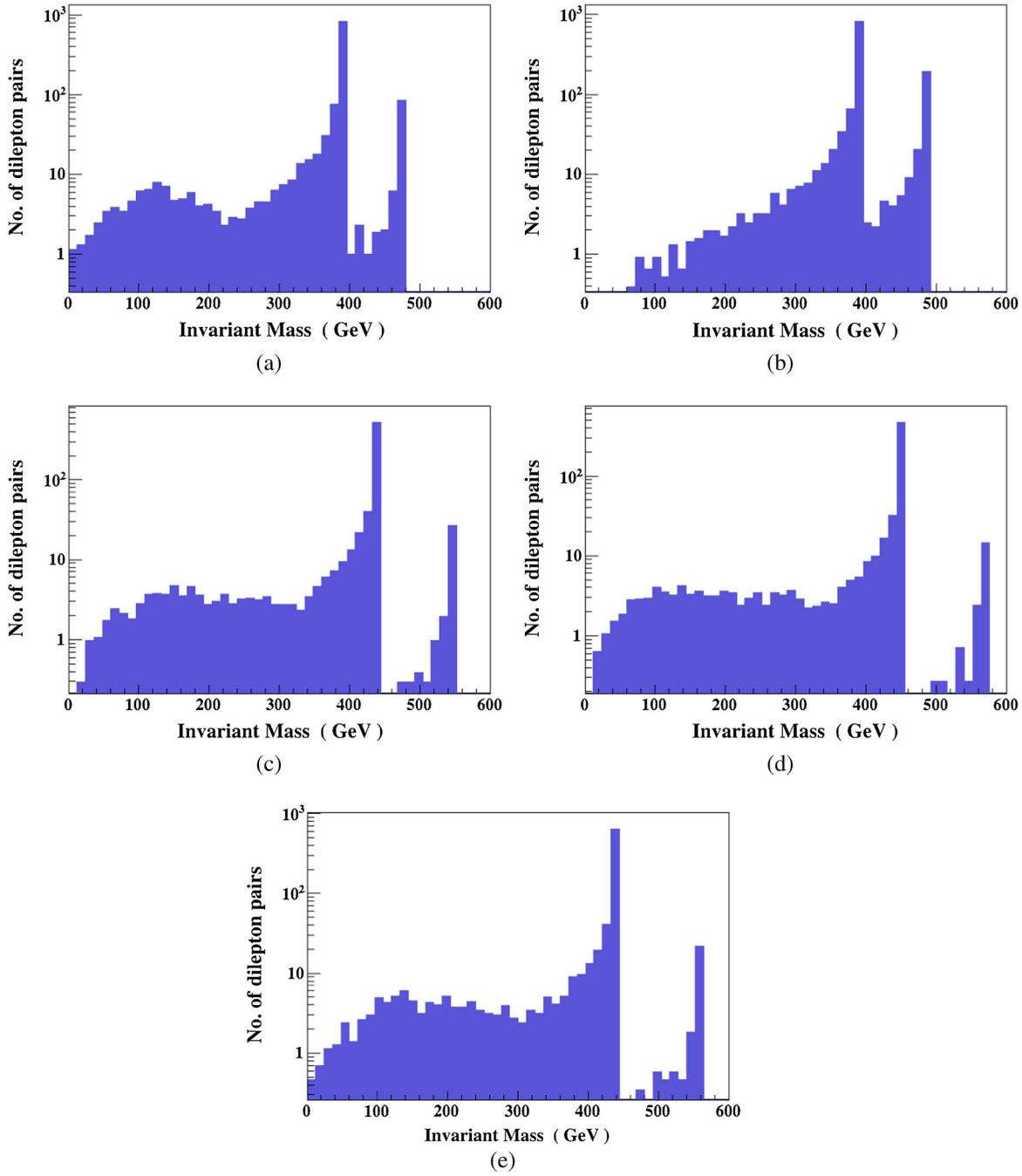

FIG. 3. Invariant mass distribution of same sign dileptons for chosen benchmark points. In (a) BP 3 and (b) BP 4 of Scenario 2 for $\alpha = 30°$. In (c) BP 3 and (d) BP 4 of Scenario 2 for $\alpha = 45°$. In (e) BP 4 of Scenario 2 for $\alpha = 60°$.

for different triplet phases are listed in Tables III, VI and IX, together with their pair-production cross sections at the LHC with $\sqrt{s} = 13$ TeV. The cross sections and branching ratios have been calculated with the help of the package FeynRules version 1.6.0) [15,16], thus creating a new Universal Feynrules Object model file in MadGraph5-aMC@NLO (version 2.3.3) [17]. Using the full machinery of scalar mixing in this model, the decay widths into various channels have been obtained.

From Tables III, VI and IX, we see that decay (55) dominates, when the masses of H_1^{++} and H_2^{++} are sufficiently separated. Also, when the phase space needed for this decay (55) is not available, the process (52) dominates over all other remaining decays. Benchmark points when decay (52) mostly dominates for $H_1^{\pm\pm}$ have been discussed in detail in Ref. [4]. Here we supplement those observations with some results for the case when decay (55) has an interesting consequence, as exemplified by Figs. 2 and 3.

TABLE X. Number of same-sign dilepton events generated at the LHC, for the benchmark points corresponding to Fig. 3. The integrated luminosity is taken to be 2500 fb^{-1}, for $\sqrt{s} = 13$ TeV.

Benchmark points, Scenario 2	No. of events at the H_2^{++} peak	No. of events at the H_1^{++} peak
BP 3 for $\alpha = 30°$	527	100
BP 4 for $\alpha = 30°$	520	139
BP 3 for $\alpha = 45°$	329	65
BP 4 for $\alpha = 45°$	287	60
BP 4 for $\alpha = 60°$	389	72

Figure 2 specifically shows the effect of enhancement of the *CP*-violating phase. We have seen in Fig. 1 that $m_{H_1^{++}} - m_{H_2^{++}}$ goes up for $\alpha \gtrsim 60°$. With this in view, the plots in Fig. 2 have been drawn for a case where both of the doubly charged scalars have appreciable coupling to same-sign dileptons. In Fig. 2(a), where the phase is lower, one notices two such dilepton pair peaks. The leptons selected for this purpose satisfy $|p_T^{\rm lepton}| > 20$ GeV, $|\eta_{\rm lep}| < 2.5$, $|\Delta R_{\ell\ell}| > 0.2$ and $|\Delta R_{\ell j}| > 0.4$ where $\Delta R^2 = \Delta\eta^2 + \Delta\phi^2$. Each peak is the result of Drell-Yan pair production of the corresponding doubly charged scalar, and the presence of two triplets is clearly discernible from the peaks themselves. In Fig. 2(b), however, with $\alpha = 65°$, one notices only the lower mass peak. This is because the decay $H_1^{++} \to H_2^{++}h$ then reigns supreme. As a result, one notices only a lower mass peak, but events in association with an SM-like Higgs are noticeable. Thus the signature of two triplets shows an interesting dichotomy of LHC signals, depending on the value of the *CP*-violating phase.

Figure 3 further elaborates the first of the above situations. The plots there bear testimony to the situation where two peaks are still visible. Table X contains the numerical values of the number of events around each peak, for five of our benchmark spectra, with varying phases. The numbers are illustrated for an integrated luminosity of 2500 fb^{-1}. The number of events correspond to a bin within ± 20 GeV of the invariant mass peak. From the table, we clearly expect several hundred events around the lower mass peak and 60–140 events around the higher one.

VI. SUMMARY AND CONCLUSIONS

We have considered a one-doublet, two-triplet Higgs scenario, with one *CP*-violating phase in the potential. It is noticed that a larger phase leads to bigger mass separations between the two doubly charged mass eigenstates, and also between the states H_1^{++} and H_2^{+}. Consequently, this scenario admits a larger region of the parameter space, when the decay $H_1^{++} \to H_2^{++}h$ opens up. When it is allowed, this decay often overrides $H_1^{++} \to H_2^{+}W^{+}$. While the role of the latter decay as a characteristic signal of such models was discussed in our earlier work, we emphasize here that the former mode leads to another interesting signal, arising from $H_1^{++} \to \ell_i^+\ell_j^+h$. This would mean that the production of SM-like Higgs together with same-sign dileptons peak at the mass of the lighter doubly charged scalar. Such a signal, too, may give us a distinctive signature of a two-triplet scenario at the LHC.

ACKNOWLEDGMENTS

This work has been partially supported by the Department of Atomic Energy, Government of India, through funding available for the Regional Centre for Accelerator-Based Particle Physics, Harish-Chandra Research Institute. We thank Subhadeep Mondal and Nishita Desai for helpful discussions.

APPENDIX

The various elements of $\mathcal{M}_{\rm neut}$, the neutral scalar mass matrix, are as follows:

$$m_{11} = 2\Big(b_{22} + \frac{1}{2}(e_{22} - h_{22})v^2 + 2(3d_{22}w_2^2 + d_{12}|w_1|^2\cos 2\alpha + 2(g+g')|w_1|^2)\Big), \tag{A1}$$

$$m_{12} = m_{21} = 2b_{12} + (e_{12} - h_{12})v^2 + 4(d_{12} + 2(g+g'))|w_1|\cos\alpha w_2, \tag{A2}$$

$$m_{13} = m_{31} = \sqrt{2}v(2t_2 + (e_{12} - h_{12})|w_1|\cos\alpha + (e_{22} - h_{22})w_2), \tag{A3}$$

$$m_{14} = m_{41} = 2d_{12}|w_1|^2\sin 2\alpha, \tag{A4}$$

$$m_{15} = m_{51} = -4(d_{12} - 2(g+g'))w_2|w_1|\sin\alpha, \tag{A5}$$

$$m_{16} = m_{61} = 0, \tag{A6}$$

$$m_{22} = 2\Big(b_{11} + \frac{1}{2}(e_{11} - h_{11})v^2 + (d_{12} + 2(g+g'))w_2^2 + d_{11}|w_1|^2(2\cos^2\alpha + 1)\Big), \tag{A7}$$

$$m_{23} = m_{32} = \sqrt{2}v(2|t_1|\cos\beta + (e_{11} - h_{11})|w_1|\cos\alpha + (e_{12} - h_{12})w_2), \tag{A8}$$

$$m_{24} = m_{42} = 4d_{12}w_2|w_1|\sin\alpha, \tag{A9}$$

$$m_{25} = m_{52} = 2d_{11}|w_1|^2 \sin 2\alpha, \tag{A10}$$

$$m_{26} = m_{62} = 2\sqrt{2}v|t_1| \sin\beta, \tag{A11}$$

$$\begin{aligned} m_{33} = \frac{1}{4}(&2a + 6cv^2 + 4|t_1||w_1| \cos(\alpha+\beta) - h_{11}w_1^2 \\ &+ 4t_2w_2 + 2(e_{12} - h_{12})|w_1| \cos\alpha w_2 \\ &+ (e_{22} - h_{22})w_2^2 - h_{11}|w_1|^2 \sin^2\alpha + e_{11}|w_1|^2), \end{aligned} \tag{A12}$$

$$m_{34} = m_{43} = \sqrt{2}(e_{12} - h_{12})v|w_1| \sin\alpha, \tag{A13}$$

$$m_{35} = m_{53} = \sqrt{2}v((e_{11} - h_{11})|w_1| \sin\alpha - 2|t_1| \sin\beta), \tag{A14}$$

$$m_{36} = m_{63} = 2|t_1||w_1| \sin(\alpha+\beta), \tag{A15}$$

$$\begin{aligned} m_{44} = 2\Big(&b_{22} + \frac{1}{2}(e_{22} - h_{22})v^2 + d_{22}w_2^2 + d_{12}|w_1|^2 \cos 2\alpha \\ &+ 2(g+g')|w_1|^2\Big), \end{aligned} \tag{A16}$$

$$m_{45} = m_{54} = 2b_{12} + (e_{12} - h_{12})v^2 + 4d_{12}|w_1| \cos\alpha w_2, \tag{A17}$$

$$m_{46} = m_{64} = 4\sqrt{2}t_2v, \tag{A18}$$

$$\begin{aligned} m_{55} = 2\Big(&b_{11} + \frac{1}{2}(e_{11} - h_{11})v^2 - 2(d_{12} - 2(g+g'))w_2^2 \\ &+ 2d_{11}|w_1|^2(2\sin^2\alpha + 1)\Big), \end{aligned} \tag{A19}$$

$$m_{56} = m_{65} = 2\sqrt{2}|t_1|v \cos\beta, \tag{A20}$$

$$\begin{aligned} m_{66} = \frac{1}{4}(&2a + 2cv^2 - 4|t_1||w_1| \cos(\alpha+\beta) \\ &- (e_{11} - h_{11})|w_1|^2 - 4t_2w_2 \\ &+ 2(e_{12} - h_{12})|w_1|w_2 \cos\alpha + (e_{22} - h_{22})w_2^2). \end{aligned} \tag{A21}$$

[1] J. C. Pati and A. Salam, Phys. Rev. D **10**, 275 (1974); R. N. Mohapatra and J. C. Pati, Phys. Rev. D **11**, 2558 (1975); G. Senjanović and R. N. Mohapatra, Phys. Rev. D **12**, 1502 (1975); W. Konetschny and W. Kummer, Phys. Lett. **70B**, 433 (1977); G. Senjanović, Nucl. Phys. **B153**, 334 (1979); R. N. Mohapatra and G. Senjanović, Phys. Rev. Lett. **44**, 912 (1980); J. Schechter and J. W. F. Valle, Phys. Rev. D **22**, 2227 (1980); T. P. Cheng and L. F. Li, Phys. Rev. D **22**, 2860 (1980); M. Magg and C. Wetterich, Phys. Lett. **94B**, 61 (1980); R. Foot, H. Lew, X. G. He, and G. C. Joshi, Z. Phys. C **44**, 441 (1989); M. Fukugita and T. Yanagida, *Physics of Neutrinos and Applications to Astrophysics* (Springer, Berlin, Germany, 2003); P. Fileviez Perez, J. High Energy Phys. 03 (2009) 142; J. Chakrabortty, A. Dighe, S. Goswami, and S. Ray, Nucl. Phys. **B820**, 116 (2009); J. Chakrabortty, Phys. Lett. **4B**, 690 (2010); G. Senjanović, Int. J. Mod. Phys. A **26**, 1469 (2011); M. Duerr, P. F. Perez, and M. Lindner, Phys. Rev. D **88**, 051701 (2013).

[2] J. Schechter and J. W. F. Valle, Phys. Rev. D **22**, 2227 (1980); M. Magg and C. Wetterich, Phys. Lett. B **94B**, 61 (1980); G. Lazarides, Q. Shafi, and C. Wetterich, Nucl. Phys. **181**, 287 (1981); R. N. Mohapatra and G. Senjanovic, Phys. Rev. D **23**, 165 (1981).

[3] H. Nishiura, K. Matsuda, and T. Fukuyama, Phys. Rev. D **60**, 013006 (1999); E. Kh. Akhmedov, G. C. Branco, and M. N. Rebelo, Phys. Rev. Lett. **84**, 3535 (2000); M. C. Chen and K. T. Mahanthappa, Phys. Rev. D **62**, 113007 (2000); S. K. Kang and C. S. Kim, Phys. Rev. D **63**, 113010 (2001); P. H. Frampton, S. L. Glashow, and D. Marfatia, Phys. Lett. B **536**, 79 (2002); Z.-Z. Xing, Phys. Lett. B **530**, 159 (2002); Z.-Z. Xing, Phys. Lett. B **539**, 85 (2002); M. Honda, S. Kaneko, and M. Tanimoto, J. High Energy Phys. 09 (2003) 028; B. R. Desai, D. P. Roy, and A. R. Vaucher, Mod. Phys. Lett. A **18**, 1355 (2003); W.-L. Guo and Z.-Z. Xing, Phys. Lett. B **583**, 163 (2004); M. Honda, S. Kaneko, and M. Tanimoto, Phys. Lett. B **593**, 165 (2004); W. Grimus and L. Lavoura, J. Phys. G **31**, 693 (2005).

[4] A. Chaudhuri, W. Grimus, and B. Mukhopadhyaya, J. High Energy Phys. 02 (2014) 060.

[5] W. Grimus, R. Pfeiffer, and T. Schwetz, Eur. Phys. J. C **13**, 125 (2000).

[6] N. G. Deshpande and E. Ma, Phys. Rev. D **18**, 2574 (1978).

[7] A. Merle and W. Rodejohann, Phys. Rev. D **73**, 073012 (2006); G. C. Branco, D. E. Costa, M. N. Rebelo, and P. Roy, Phys. Rev. D **77**, 053011 (2008); S. Choubey, W. Rodejohann, and P. Roy, Nucl. Phys. **B808**, 272 (2009); **B818**, 136(E) (2009); B. Adhikary, A. Ghosal, and P. Roy, J. High Energy Phys. 10 (2009) 040; H. Fritzsch, Z. Z. Xing, S. Zhou, J. High Energy Phys. 09 (2011) 083; G. Blankenburg and D. Meloni, Nucl. Phys. **B867**, 749 (2013); L. Wang and X. F. Han, Phys. Rev. D **87**, 015015 (2013); P. O. Ludl and W. Grimus, J. High Energy Phys. 07 (2014) 090; 10 (2014) 126(E); J. Liao, D. Marfatia, and K. Whisnant, Nucl. Phys. **B900**, 449 (2015); H. Fritzsch, Mod. Phys. Lett.

A **30**, 1550138 (2015); L. M. Cebola, D. Emmanuel-Costa, and R. G. Felipe, Phys. Rev. D **92**, 025005 (2015); L. Lavoura, J. Phys. G **42**, 105004 (2015); A. Ghosal and R. Samanta, J. High Energy Phys. 05 (2015) 077; P. O. Ludl and W. Grimus, Phys. Lett. B **744**, 38 (2015).

[8] P. H. Frampton, S. L. Glashow, and D. Marfatia, Phys. Lett. B **536**, 79 (2002); W. Grimus and L. Lavoura, J. Phys. G **31**, 693 (2005).

[9] J. Beringer *et al.* (Particle Data Group), Phys. Rev. D **86**, 010001 (2012).

[10] G. L. Fogli, E. Lisi, A. Marrone, D. Montanino, A. Palazzo, and A. M. Rotunno, Phys. Rev. D **86**, 013012 (2012).

[11] F. P. An *et al.* (Daya Bay Collaboration), Phys. Rev. Lett. **108**, 171803 (2012).

[12] J. K. Ahn *et al.* (RENO Collaboration), Phys. Rev. Lett. **108**, 191802 (2012).

[13] N. Chakrabarty, U. K. Dey, and B. Mukhopadhyaya, J. High Energy Phys. 12 (2014) 166; N. Chakrabarty, arXiv: 1511.08137 [Phys. Rev. D (to be published)].

[14] M. A. Schmidt, Phys. Rev. D **76**, 073010 (2007); J. Elias-Miro, J. R. Espinosa, G. Giudice, G. Isidori, A. Riotto, and A. Strumia, Phys. Lett. B **709**, 222 (2012); E. J. Chun, H. M. Lee, and P. Sharma, J. High Energy Phys. 11 (2012) 106.

[15] N. D. Christensen and C. Duhr, Comput. Phys. Commun. **180**, 1614 (2009).

[16] C. Degrande, C. Duhr, B. Fuks, D. Grellscheid, O. Mattelaer, and T. Reiter, Comput. Phys. Commun. **183**, 1201 (2012).

[17] J. Alwall, R. Frederix, S. Frixione, V. Hirschi, F. Maltoni, O. Mattelaer, H. S. Shao, T. Stelzer, P. Torrielli, and M. Zaro, J. High Energy Phys. 07 (2014) 079.